Journal of Materials Chemistry B

Accepted Manuscript

ROYAL SOCIETY OF CHEMISTRY

www.rsc.org/materialsB

Injectable in situ forming poly(L-glutamic acid) hydrogels for cartilage tissue engineering

Shifeng Yan,[*ac] Xin Zhang,[a] Kunxi Zhang,[a] Hao Di,[a] Long Feng,[a] Guifei Li,[a] Jianjun Fang,[a] Lei Cui, [*b] Xuesi Chen,[*d] Jingbo Yin[*a]

[a]*Department of Polymer Materials, Shanghai University, 333 Nanchen Road, Shanghai 200444, People's Republic of China. E-mail*: yansf@staff.shu.edu.cn; jbyin@oa.shu.edu.cn

[b]*Medical Science and Research Center, Beijing Shijitan Hospital, Capital Medical University, 10 Tieyi Road, Beijing 100038, People's Republic of China. E-mail*: cuileite@yahoo.com.cn

[c]*State Key Laboratory of Molecular Engineering of Polymers, Fudan University, Shanghai 200433, People's Republic of China.*

[d]*Key Laboratory of Polymer Ecomaterials, Changchun Institute of Applied Chemistry, Chinese Academy of Sciences, 5625 Renmin Street, Changchun 130022, People's Republic of China. E-mail*: xschen@ciac.jl.cn

**Corresponding Author - jbyin@oa.shu.edu.cn*

Abstract

The injectable, in situ forming hydrogels have exhibited many advantages in regenerative medicine. This study presented a novel design of poly(L-glutamic acid) injectable hydrogels via self-crosslinking of adipic dihydrazide (ADH)-modified poly(L-glutamic acid) (PLGA-ADH) and aldehyde-modified poly(L-glutamic acid) (PLGA-CHO), and investigated their potential in cartilage tissue engineering. Both the hydrazide modification degree of PLGA-ADH and the oxidation degree of PLGA-CHO could be adjusted by the amount of activators and sodium periodate, respectively. Experiments revealed that the solid content of the hydrogels, $–NH_2$/–CHO molar ratio, and oxidation degree of PLGA-CHO had a great effect on the gelation time, equilibrium swelling, mechanical properties, microscopic morphology, and in vitro degradation of the hydrogels. Encapsulation of rabbit chondrocytes within hydrogels showed viability of the entrapped cells and cytocompatibility of the injectable hydrogels. A preliminary study exhibited injectability and rapid in vivo gel formation, as well as mechanical stability, cell ingrowth, and ectopic cartilage formation. These results suggested that the PLGA hydrogel had potential as an injectable cell delivery carrier for cartilage regeneration and could serve as a new biomaterial for tissue engineering.

Keywords: Tissue engineering, Poly (L-glutamic acid), Injectable hydrogel, Self-crosslinking

1. Introduction

Human cartilage has a limited capacity to repair itself due to avascularity and a poor supply of repair cells in this tissue.[1] Tissue engineering has emerged as a promising approach in the treatment of damaged cartilage and a potential solution to the severe shortage of donor tissue.[2] In this approach, a three-dimensional scaffold serves as a temporary artificial extracellular matrix (ECM), supporting the growth, proliferation and differentiation of incorporated chondrocytes and/or progenitor cells.[3] As an important class of scaffolds, hydrogels are crosslinked, hydrophilic, polymeric networks capable of imbibing large amount of water or biological fluids, which mimic hydrated native cartilage tissue.[4]

From a clinical perspective, the injectable, in situ forming hydrogel systems are highly desirable since the precursors containing therapeutic drugs and cells can be applied via a minimally invasive procedure. After injection of a precursor solution, irregular surgical defects are completely filled with in situ formed hydrogels.[3-6]

Various methods, including physical or chemical crosslinking, have been employed to prepare injectable hydrogels. Physical crosslinking injectable hydrogels are spontaneously formed by weak secondary forces such as electrostatic interactions,[7] stereocomplexation,[8,9] hydrophobic interactions,[10] and hydrogen bonding between water soluble polymer chains.[11] However, the major handicaps of these physical crosslinking injectable hydrogels are the low stability and low mechanical properties, diffusion of hydrogel precursors to the surrounding tissue and premature gelation inside the delivery needle/catheter.[12] Compared with physical crosslinking hydrogels, the chemical crosslinking hydrogels exhibit higher stability and better mechanical properties. Chemical bonds can be in situ formed and covalently crosslinked, using photopolymerization of their custom-made monomers,[13] or chemical crosslinking by crosslinkers.[6,14] Thus, some cytotoxic reagents, including photosensitizers, crosslinking agents are inevitably introduced into the chemical crosslinking hydrogel systems, which is the major obstacle in the use of injectable hydrogel systems. What's more, prolonged irradiation that may induce cell death is required for

photopolymerization, thus limiting their applications.[15]

Recently, intermacromolecular in situ chemical crosslinking systems using Schiff base reaction have been investigated because of their various advantages, such as avoidance of chemical crosslinking agents and easy control of reaction rate under mild condition. Several natural polysaccharides such as alginate,[6] dextran,[16] chondroitin sulphate,[17] and hyaluronic acid[14] were partially oxidized and employed for the preparation of hydrogels as cell carriers for tissue engineering applications. However, the natural polysaccharides exhibit batch-to-batch variation, offer limited control over chemical structure, molecular weight, and degradation profiles.[18] Besides, partially oxidation often leads to depolymerization of polysaccharides and substantial deterioration of mechanical strength.[19]

Alternatively, synthetic polymer-based scaffolds were developed as a response to the need for more tunable materials for tissue engineering. Poly(vinyl alcohol) have been used for the preparation of hydrogels via the Schiff base reaction. However, the lack of degradable linkages could lead to trapping of the cells with no evolution of void space around them, thus, physically preventing their proliferation.[20] Most of synthetic polyesters are absence of tailorable and functional groups for modification and crosslinking, restricting their use in injectable hydrogels formed through the Schiff base reaction. Also, most of synthetic polyesters inherently lack of the biological recognition motifs required for seeded cell interaction and induce immune and/or inflammatory responses likely related to the release of polymer degradation products.[2,21] Poly(L-glutamic acid) (PLGA), a synthetic polypeptide, is composed of naturally occurring L-glutamic acid linked together through amide bonds and exhibits the advantages of nontoxicity, hydrophilicity, biodegradability and avoiding antigenicity or immunogenicity.[22] As a promising candidate for drug carrier and tissue engineering scaffold, PLGA has attracted considerable interest in recent years.[22-24] However, few reports have been found regarding that PLGA served as injectable hydrogel in tissue engineering. Developing injectable in situ forming PLGA hydrogels suitable for tissue regeneration remains a challenge.

The present work demonstrated a strategy to develop injectable in situ forming

PLGA hydrogels. The modification of PLGA was described. The hydrogels were investigated in term of gelation time, swelling behavior, degradation, rheological properties and micromorphology. Chondrocytes were encapsulated within the hydrogels to evaluate their cytocompatibility and the ability to induce ectopic cartilage formation in vivo.

2. Materials and methods

2.1 Materials

Poly (L-glutamic acid) (PLGA, M_v=6.0×10^4) was prepared by removal of γ-benzyl protection groups of poly(γ-benzyl-L-glutamate) (PBLG), which was synthesized by the ring-opening polymerization of the N-carboxyanhydride (NCA) of γ-benzyl-L-glutamate in our laboratory. 1-ethyl-3-(3-dimethylaminopropyl) carbodiimide hydrochloride (EDC), N-hydroxysuccinimide (NHS), and 1-hydroxy-benzotriazole hydrate (HOBt) were purchased from Covalent Chemical Technology Co., Ltd (Shanghai, China). Adipic dihydrazide (ADH), sodium periodate ($NaIO_4$), hydroxylamine hydrochloride, ethylene glycol and 3-amino-1,2-propanediol were purchased from Shanghai Darui Fine Chemical Co., Ltd. (Shanghai, China). All other chemicals were of analytical grade and were used without further purification.

2.2 Synthesis of hydrazide-modified PLGA (PLGA-ADH)

For the preparation of hydrazide-modified PLGA (PLGA-ADH), PLGA was dissolved in distilled water to obtain a 0.25wt % solution, and then reacted with ADH in the presence of EDC and NHS. The molar ratio of EDC to NHS was set at 1:1. The molar ratio of ADH to –COOH of PLGA was changed from 0.2 to 12, while the molar ratio of EDC to –COOH of PLGA was 0.2, 0.5, 1, 2 and 3, respectively. The pH of the reaction mixture was adjusted to 5.5 by the addition of 0.1 M NaOH or HCl solution. The reaction was allowed to continue at room temperature for 24 h. Then, the reaction solution was exhaustively dialyzed against deionized water followed by lyophilization.

2.3 Synthesis of aldehyde-modified PLGA (PLGA-CHO)

For the preparation of aldehyde-modified PLGA (PLGA-CHO), PLGA was dissolved in distilled water to obtain a 0.25wt % solution, and then reacted with 3-amino-1,2-propanediol in the presence of EDC and HOBt. The molar ratio of –COOH of PLGA to 3-amino-1,2-propanediol was set at 1:6. While the molar ratio of EDC: HOBt: –COOH was 3:1:1. The oxidation reaction proceeded at room temperature in the dark for 3h. The pH of the reaction mixture was adjusted to 5.5 by the addition of 0.1 M NaOH or HCl solution. The reaction was allowed to continue at room temperature for 24 h. The dried diol-modified PLGA (PLGA-OH) was obtained by exhaustive dialyzation against deionized and subsequent freeze-drying.

A solution of PLGA-OH (0.1wt %) was oxidized in $NaIO_4$ solution. The oxidation reaction proceeded at room temperature in the dark for 5min. The reaction was stopped by adding excess amount of ethylene glycol in a molar ratio of –OH to $NaIO_4$ of at least 3. Then the solution was dialyzed immediately against distilled water for 3 days. The final purified aldehyde-modified PLGA (PLGA-CHO) product was obtained by freeze-drying.

2.4 Preparation of PLGA hydrogels

PLGA-ADH and PLGA-CHO were used as precursors to prepare PLGA hydrogels. Various factors that might affect the properties of hydrogels were considered during the preparation of PLGA hydrogels, including solid content, $–NH_2$/–CHO molar ratio and oxidation degree of PLGA-CHO. PLGA-ADH and PLGA-CHO were separately dissolved in phosphate buffer (PBS) solution (pH 7.4). Then two solutions were gently mixed to form the resultant hydrogels.

2.5 Characterization of polymers

The modification of PLGA was confirmed by ^{1}H NMR (AV 500 MHz) and FTIR spectrophotometer (AVATAR 370, Nicolet, USA). The ^{1}H NMR spectra were obtained by an AV 500 NMR from BRUKER to analyze the conjugation efficiency of ADH to

the PLGA side chains by comparing the peaks from the groups of ADH and PLGA. Deuterated water (D_2O) was used as solvent for all the samples.

The FTIR spectra were recorded using a FTIR spectrophotometer (AVATAR 370, Nicolet, USA) in the region of 4000−500 cm^{-1} using a KBr pellet method. PLGA, PLGA-ADH, and PLGA-CHO were determined with the KBr tablet of each polymer.

The oxidation degree of PLGA-CHO, i.e. percentage of oxidized PLGA repeating units, was determined by measuring the aldehyde content using hydroxylamine hydrochloride titration method.[25] Some amount of lyophilized PLGA-CHO was dissolved in 25 mL of 0.25 mol/L hydroxylamine hydrochloride solution (pH adjusted to 4.5) containing 0.002 wt % methyl orange reagent. The mixture was stirred at room temperature for 24 h. The conversion of aldehydes into oximes was followed by titration of the released hydrochloric acid with 0.1 mol/L sodium hydroxide solution until the red-to-yellow end point was achieved. The change of pH with the volume of added sodium hydroxide solution was recorded. The related reactions and calculation formula are as follows:

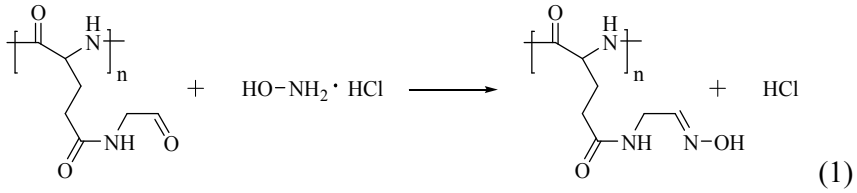

(1)

$$HCl + NaOH = NaCl + H_2O \quad (2)$$

$$\Delta V \times n_{NaOH} = n$$

$$W = n \times M_{PLGA\text{-}CHO} + m \times M_{PLGA\text{-}OH}$$

$$\text{Oxidation degree (100\%)} = n/(n+m) = n/[(W - n \times M_{PLGA\text{-}CHO})/M_{PLGA\text{-}OH} + n]$$

where ΔV is the consumed volume of sodium hydroxide solution, in mL; n the amount of –CHO groups in the PLGA-CHO sample, in mol; W the weight of PLGA-CHO, in grams; $M_{PLGA\text{-}CHO}$, equaling to 171, is the molecular weight of aldehyde-modified PLGA repeating units, in g/mol; and $M_{PLGA\text{-}OH}$, equaling to 202, is the molecular weight of glycol-modified PLGA repeating units, in g/mol.

2.6 Characterization of hydrogels

X-ray diffraction patterns were analyzed using a diffactometer (D/MAX2550,

Rigaku), with CuKα radiation at a voltage of 40 kV and 30 mA. The samples were scanned between 2θ = 5−40° with a scanning speed of 5°/min.

The thermal gravimetric analysis was examined by means of thermogravimetry with a heating rate of 10 °C/min in nitrogen atmosphere on TA Q-500 instruments.

Gelation time was measured as described previously.[26] 100 μL of PLGA-ADH solution was injected into 100 μL of PLGA-CHO solution with stirring at 200 rpm using a magnetic stir bar on a Petri dish. The time until the mixture became a globule was regarded as gelation time. The experiments were performed in triplicate.

Morphology of the lyophilized gel was examined by scanning electron microscopy (SEM). The hydrogels were immersed into liquid nitrogen and lyophilized at room temperature. The cross-section of hydrogels was gold-coated and viewed using a microscope (JXA-840, JEOL).

For the swelling test, the hydrogels prepared at various conditions were immersed in both PBS buffer solution and high glucose Dulbecco's modified Eagle's medium (DMEM) and kept at 37 °C for 2 days until equilibrium of swelling had been reached. Fully swollen hydrogels were weighed (W_s) immediately after the excess of water lying on the surfaces was absorbed with filter paper. Dry hydrogels were weighed (W_d) after quickly frozen at −80 °C and lyophilized. The experiments were performed in triplicate and the swelling ratio was expressed as $(W_s - W_d)/W_d$.

Degradability of the PLGA hydrogels was evaluated by the mass change of the dried samples after their incubation in 1 M phosphate-buffered saline (PBS) (pH=7.4, 37°C) without and with 0.25mg/ml papain (Ourchem, Sinopharm Chemical Reagent Co., Ltd.). The solution was replaced every day by a fresh solution. At the indicated time point, samples were carefully withdrawn from the medium and thoroughly rinsed with distilled water, and freeze-dried for 24 h to remove excess water. The weight remaining was calculated using the following equation:

Weight remaining (%) = $W_t / W_0 \times 100\%$,

where W_0 and W_t are the weights of the dried hydrogels before and after degradation for a specific time interval, respectively.

Rheological experiments were carried out with a rheometer (AR2000, TA

Instruments, U.S.A.) using parallel plates (diameter, 30 mm) configuration at 37 °C in the oscillatory mode. To study the viscoelastic behavior of the hydrogels, the frequency sweep test was performed, which covered a range of frequencies from 1 to 100 rad/s at controlled regular strain of γ = 0.01. The hydrogels were precured at 37 °C for 8 h before testing. The storage modulus G', loss modulus G'', and dynamic viscosity η were obtained with respect to frequency.

2.7 Chondrocyte culture and viability analysis

All animal experiment procedures were approved by the Institutional Animal Care and Use Committee of Shanghai Jiaotong University. Primary auricular chondrocytes were isolated enzymatically from ears of New Zealand rabbits (2.5−3 kg). Cartilage tissue was diced into small pieces and digested with 0.2% collagenase (Serva, Heidelberg, Germany) at 40 °C for 8 h and cultured in high glucose Dulbecco's modified Eagle's medium (DMEM) containing 10 vol % fetal bovine serum (FBS), and 1 wt % of penicillin-streptomycin. Cells at passage less than 2 were collected for cell seeding.

Chondrocytes were encapsulated in the injectable hydrogels under sterile condition. Briefly, PLGA-ADH and PLGA-CHO solution with the concentration of 6 wt % in phosphate buffered saline (PBS) were sterilized respectively by filtration through filters with a pore size of 0.22 μm. Chondrocytes were first suspended in 10 mL of PLGA-ADH solution at a concentration of 1×10^6 cells/mL, then 10 mL of PLGA-CHO solution was added. The mixture solution was immediately injected into 24-well plate before the formation of hydrogels, and then formed cell/hydrogel matrix was cultured in 1 ml of complete DMEM at 37 °C and 5% CO_2 in humidified incubators.

The effect of hydrogels on cell survival was studied using a live−dead assay. At 3, 9, 4 and 21 d, the hydrogel constructs were rinsed with PBS and stained with fluorescein diacetate/propidium iodide (FDA/PI) using the live−dead assay kit (Invitrogen), according to the manufacturers' instructions. The viability of encapsulated cells was observed under a fluorescence microscope (Leica). As a result

live cells fluoresce green and the nuclei of dead cells fluoresce red.

The morphology of the chondrocytes in the hydrogels was observed using a Phenom G2 pro desktop SEM equipped with a cold stage (temperature controlled sample holder, TCSH). After in vitro culture for indicated times, the cell/hydrogel constructs were fixed with glutaraldehyde for 8 h, the samples were then placed on the sample holder and cooled from room temperature to −20 °C at the rate of −20 °C/min for cryo-microscopy.

2.8 Subcutaneous injection of PLGA hydrogels into nude mice

After sterilization by filtration through filters with a pore size of 0.22 μm, the bi-component precursors of the hydrogels containing PLGA-ADH and PLGA-CHO solution were injected subcutaneously on the back of the mice using dual-syringe. Each injection contained 1 mL of PLGA-ADH solution (6 wt %) with suspended chondrocytes and 1 mL of PLGA-CHO solution (6 wt %) in PBS at final cell density of 1×10^6/mL.

For comparison, the suspensions of chondrocytes with same volume and cell density were also injected subcutaneously on the back of the mice. Following the injection, animals were euthanized at 12 weeks for sample harvesting.

Samples were fixed in neutral buffered formalin, embedded in paraffin, sectioned (5 mm thick) followed by hydration in ethanol solutions of decreasing concentration and observed histologically by safranin-O and toluidine blue staining, respectively. Expression of COL II in the engineered cartilage was also examined by immunohistochemical staining.

2.9 Statistical analysis

The experimental data from all the studies were expressed as means ± standard deviation (SD). Single factor analysis for variance (ANOVA) was used to assess the statistical significance of the results. Statistical significance was set to a p value $\leq$ 0.05.

3. Results and discussion

3.1 PLGA modification and characterization

Airming to design a biomimetic injectable hydrogel for tissue engineering, the material should be carefully selected and tuned to create extracellular matrix (ECM) mimicking microenvironments and meet the requirement of the native target tissue.[27] Both natural and synthetic polymers can be used for the production of hydrogels. Natural polysaccharides and proteins mimic many features of ECM, many of them demonstrate adequate biocompatibility and biodegradability. However, the naturally derived polymers show disadvantage of low mechanical properties, pathogenicity, batch-to-batch variation, and limited availability.[28] Synthetic polymers, especially biodegradable multiblock polyesters have been explored as injectable thermosensitive hydrogels, such as the block copolymers of poly(*ε*-caprolactone),[29] polylactide,[30] poly(lactic acid-*co*-glycolic acid)[31] with poly(ethylene glycol) (PEG). A serious problem is lack of intrinsic biological activity, leading to in vivo foreign body reactions.[32]

In contrast, poly(L-glutamic acid) (PLGA) has received great interest because of a more regular arrangement and a smaller diversity of amino acid residues than those derived from natural proteins. As a kind of synthetic polypeptides, PLGA shows excellent cytocompatiblity, high hydrophilicity and suitable biodegradability.[33] With abundant carboxylic acid groups in side-chain, PLGA's propertities could be tailored by simply side-chain modification.

In the work presented here, we tried to convert the -COOH groups into reactive ADH and aldehyde groups.

3.1.1 Synthesis and characterization of PLGA-ADH

EDC and NHS were used as the carboxylic acid activators to realize the reaction between PLGA and ADH, as shown in Fig. 1a. An active ester with the NHS was formed, which was highly reactive with amines. Aminolysis of NHS-active esters with hydrazine groups of ADH resulted in a stable amide bond. Thus, a two-step procedure allowed PLGA to be effectively modified with highly reactive hydrazide

groups.

Synthesis of PLGA-ADH was confirmed by FTIR, TGA and ^{1}H NMR spectra. Fig. 1b demonstrates FTIR spectra of PLGA, ADH and PLGA-ADH. For PLGA, the characteristic absorption peaks at 1758, 1657 and 1534cm^{-1} were attributed to the stretching vibration of C=O stretch band from COOH groups, amide I and II vibration bands, respectively.[34] ADH also presented the characteristic amide I and II bands at 1690 and 1569cm^{-1}, respectively. After modification of PLGA with ADH, new amide bonds were formed between –COOH groups from PLGA and –NH_2 groups from ADH. The modification was monitored by observation of new peaks at 1684 and 1571 cm^{-1}. The former peak could be ascribed to the superposition of vibrations of C=O from residue –COOH groups and amide I vibration of the original and newly generated amide groups, while the latter could be ascribed to the superposition of amide II vibration from the amide groups in both main and side chains of PLGA-ADH.

The representative ^{1}H NMR spectra of PLGA, ADH, and PLGA-ADH are presented in Fig. 1c. The alphabetically labeled peaks were assigned to the corresponding protons shown in inset scheme. The peaks at 1.78, 1.88, 2.11, and 4.16 ppm were characteristic of proton peaks of PLGA, which was in accordance with previous result.[35] The resonance peak at 4.16 ppm was attributed to the protons binding to the α-carbon of L-glutamic acid (1H, α-CH). The modification of PLGA with ADH was confirmed by new peaks at 1.46 ppm, corresponding to the methylene protons (4H, CH_2CH_2) of ADH. The degree of PLGA-ADH modification was determined from the relative peak area at 1.46 and 4.16 ppm. With the increase in ADH and EDC amount, the peak area at 1.46 ppm increased accordingly, indicating the increase of ADH modification degree (Fig. 1d and 1e). The degree of ADH modification onto PLGA increased gradually from 28 to 52%, when ADH/PLGA (–COOH of PLGA, similarly hereinafter) molar ratio increased from 0.2 to 12 (EDC/PLGA=1). By comparison, a more significant increase of ADH modification degree was observed upon increasing EDC amount. With the increase of EDC/PLGA molar ratio from 0.2 to 3 (ADH/PLGA=3), the degree of ADH modification increased from 18% to 51%. Meanwhile, the viscosity-average molecular weight (M_v) increased

gradually from 4.0×10^5 to 4.9×10^5.

3.1.2 Synthesis and characterization of PLGA-CHO

The synthesis of aldehyde-modified PLGA (PLGA-CHO) by chemical modification of carboxylic acid groups was carried out in two steps,[20] as shown in Fig. 2a. At first, EDC and HOBt were used as activators to realize reaction between carboxylic acid group in PLGA and amino group in 3-amino-1,2-propanediol. The yielded 1,2-diol modified PLGA (PLGA-OH) was then treated with $NaIO_4$ to generate the aldehyde groups in the final PLGA-CHO.

As described above, PLGA showed the characteristic absorption peaks at 1758, 1657 and 1534cm^{-1}, respectively (Fig. 2b). After functionalization with 3-amino-1,2-propanediol, a new absorption band at 1630 cm^{-1} was detected in the spectrum of PLGA-OH. Compared with the absorption of PLGA-OH, a new inconspicuous absorption band at 1763 cm^{-1} was detected in the spectrum of PLGA-CHO, corresponding to the aldehyde symmetric vibration,[14,25,36] which reflected effective aldehyde modification of PLGA.

Thermal stabilities of PLGA, PLGA-OH and PLGA-CHO were measured using TGA analysis, as shown in Fig. 2c. Before modification, PLGA exhibited decomposition temperature of 265°C at the maximum decomposition rate. After functionalization with 3-amino-1,2-propanediol, thermal stability was greatly enhanced with higher decomposition temperature and slower thermal decomposition rate, which might be ascribed to the formation of stable amide bonds, strong hydrogen bonding interaction of hydroxyl groups introduced onto molecular chain, as well as the increasing molecular weight. After further oxidation with $NaIO_4$, a decrease of thermal stability was detected. However, compared with PLGA, PLGA-CHO exhibited slightly increased thermal decomposing temperature.

Fig. 2d shows the ^{1}H NMR spectra of PLGA, 3-amino-1,2-propanediol and PLGA-OH. For PLGA, the peak at 4.16 ppm was attributed to the protons binding to the α-carbon of L-glutamic acid (1H, α-CH). For 3-amino-1,2-propanediol, two multiple peaks located at 2.50 and 2.60 ppm were assigned to methylene protons being adjacent to amino group. The resonance peaks for another methylene and

methine protons appeared at 3.43, 3.50 and 3.58 ppm. The ^{1}H NMR spectrum of PLGA-OH displayed the characteristic peaks for both PLGA and 3-amino-1,2-propanediol. However, the two multiple peaks for methylene protons shifted to 3.13 and 3.23 ppm, indicating the linkage of 3-amino-1,2-propanediol to PLGA. According to the calculation of relative peak area, the diol-modification degree was about 98%, almost complete substitute of carboxyl groups. Fig. 2e exhibites the ^{1}H NMR spectra of diol-modified PLGA before and after oxidation. The two spectra were similar. The only difference was that a small peak appeared at 4.98 ppm for PLGA-CHO, which was ascribed to methylene protons adjacent to aldehyde groups transformed from oxidation cleavage of vicinal diol groups presented in PLGA-OH.

The oxidation degree of PLGA-CHO was defined as the number of oxidized residues per 100 PLGA repeating units and quantified by using hydroxylamine hydrochloride titration potentiometric, as described elsewhere for some oxidized polysaccharides.[17] The change of pH value with added sodium hydroxide solution is shown in Fig. 2f. The equivalent volume of sodium hydroxide solution could be determined by peaks of the first derivative of the titration curve. Fig. 2g displays the theoretical degree of oxidation, which reflected the molar ratio of sodium periodate per initial diol groups in PLGA-OH, and the obtained degree of oxidation calculated by the assay with hydroxylamine hydrochloride. As expected, the oxidation degree of PLGA-CHO increased as the amount of added periodate increased. Moreover, the degree of oxidation obtained experimentally for PLGA-CHO was very close to the theoretical values. So oxidation degree could be readily controlled by the mole equivalent of sodium periodate used in each reaction.

The viscosity average molecular weights (M_v) before and after modification are also shown in Fig. 2g. Compared with PLGA, the diol-modified PLGA showed an increase of about 33% in M_v, indicating that 3- amino-1, 2-propanediol was successfully grafted onto the molecular chains of PLGA. The molecular weight decreased with the increasing amount of oxidant, which could be ascribed to the oxidation of vicinal diol groups and the partial fracture of the molecular chain.[6,37]

It was reported that polysaccharide oxidation often led to serious decrease of molecular weight because of cleavage of the glycosidic bonds of the polymer backbone.[6,38] For PLGA-OH, the oxidation was mainly limited to the diol structure on the side chain, and the destruction of PLGA backbone was not serious.

3.2 In situ formation and gelation time of PLGA hydrogels

Hydrogel gelation is commonly accomplished by physical or chemical cross-linking. Compared with physical cross-linking systems, the chemical cross-linking counterparts exhibited strong mechanical properties and high stability. However, toxic reagents, such as the photoinitiator or organic solvent, are often required for hydrogel formation.[6]

Recently, intermacromolecular in situ chemical crosslinking systems using Michael addition,[39] enzymatic reaction[40] and schiff base reaction[41] have been widely investigated. In particular, schiff base reaction has various advantages, such as biocompatibility and easy control of reaction rates under mild condition, which was proved as an efficient way to prepare biocompatible injectable hydrogels for tissue engineering.

Here, mixing PLGA-ADH and PLGA-CHO together resulted in schiff base crosslinking of the hydrogels. As shown in Fig. 3a, the mechanism of gelation was attributed to the Schiff base reaction between hydrazide groups and aldehyde groups with the formation of hydrazone bonds.[37]

Considering insolubilization of PLGA-CHO with high oxidation degree probably caused by strong hydrogen bond between the aldehyde group and diol groups, PLGA-ADH with high modification of 45% and PLGA-CHO with oxidation degree of 15% were selected as a pair of the component polymers for the hydrogels by aiming to ensure relatively high crosslinking density and strength for hydrogel systems. For comparison, PLGA-CHO with the oxidation degrees of 10 and 20% was also used.

Fig. 3b shows a photograph of the in situ formation of hydrogels using dual syringes. Syringes (A) and (B) were filled with PBS solution of PLGA-ADH and

PLGA-CHO, respectively. The mixing of the component polymer solutions inside the needle led to rapid crosslinking in between two component polymers and the formation of transparent and soft hydrogels.

The formation of crosslinking structure of the hydrogels could be studied by FTIR and TGA. Fig. 3c shows the FTIR diffraction patterns of the hydrogels and the component polymers. For PLGA hydrogel, the vibration peaks at 1763cm^{-1} for aldehyde groups obviously decreased. And a new vibration peak appeared at 1647 cm^{-1}, ascribed to the superposition of vibrations of C=O, amide I and II groups, as well as newly-formed C=N groups in between the polymer chains.[38]

The thermal decomposition behaviors of the PLGA hydrogel and components polymers were investigated by TGA, as presented in Fig. 3d. Compare with PLGA-CHO and PLGA-ADH, the PLGA hydrogel showed an increase in thermal stability with higher decomposition temperature and less weight loss rate at 700℃, which indicated the chemical crosslinking between PLGA-ADH and ALG-CHO and the formation of a stable network structure.

A suitable injectable hydrogel should be easily injected and rapidly crosslinked in a reasonable time.[42] Therefore, the gelation time plays a key role in the design of injectable scaffolds and fulfilling the clinical requirements. It should be short enough to prevent the unwanted diffusion of gel precursors. However, excessively rapid and premature gelation may lead to needle clogging or an increase in the viscosity of the injectable solution.[43]

Fig. 3e shows the effect of solid content on the gelation time of the PLGA hydrogels. No formation of stable gel occurred when the precursor polymer solutions with a concentration less than 2 wt% were employed, which was ascribed to low crosslinking density and incomplete network structure. So a minimum solid content was essential for rapid gelation. The gelation time was reduced drastically from 24 to 9s, as the solid content increased from 3 to 6 wt%. By increasing the solid content, the number of reactive groups per unit volume and crosslinking density was increased, resulting in the accelerated gelation and short gelation time.

The molar ratio of $-NH_2$ to –CHO also greatly affected the gelation time. As shown

in Fig. 3f, with increasing amount of PLGA-ADH in the hydrogels, the gelation time first decreased from 20s and reached the minimum value of 11s, then gradually increased to 26s. The greatly excessive groups for $–NH_2$ or –CHO resulted in quite a number of un-reacted residual groups and a slow gelation rate. Tan et al. reported that, the gelation time of hydrogels based on N-succinyl-chitosan (S-CS) and aldehyde hyaluronic acid (A-HA) first decreased, and then increased with increasing ratios of S-CS, which was in accordance with the current result.[14]

The influence of oxidation degree of PLGA-CHO on the gelation time of the PLGA hydrogels is demonstrated in Fig. 3g. The gelation time gradually decreased, when the oxidation degree increased from 10 to 20%, ascribed to the more aldehyde groups and increasing crosslinking density of the hydrogel systems.

3.3 Swelling behavior and degradation of PLGA hydrogels

Swelling ratio is an important parameter that represents the efficiency of oxygen and nutrient transfer within a scaffold.[44] Many of their other properties and applicability of hydrogels are strongly influenced by the swelling property.[45] Park H et al. reported that chondrogenic differentiation in oligo(poly(ethylene glycol) fumarate) (OPF) hydrogel composites was affected by the swelling ratio (or mesh size) of surrounding hydrogels, which could be used as a novel strategy for controlling the differentiation of mesenchymal stem cells (MSCs).[46]

The swelling ratios of the PLGA hydrogels swollen in different mediums to reach equilibrium are shown in Fig. 4a, b and c. All of the hydrogels showed high swelling ratio, ranging from 12 to 30 under different conditions. It was previously reported that increasing the polymer concentration exhibited a significant effect on water uptake capacity of the hydrogels and the absolute value of equilibrium swelling ratio.[47] At higher concentrations, aggregation of macromolecule chains resulted in greater extent of side reactions and higher crosslinking density, which impeded the process of swelling of the hydrogels. While the hydrogels with low solid content ($\leqslant$3 wt%) were instability and soluble in aqueous solution because of low crosslinking density. As expected, the swelling ratio decreased drastically from 28~30 to 12~15 in both PBS

and DMEM, when the solid content increased from 4 to 6 wt % (Fig. 4a). The influence of $–NH_2$ to –CHO molar ratio on swelling ratio of the hydrogels is shown in Fig. 4b. The hydrogel with the $–NH_2$/–CHO molar ratio of 1:2 became soluble in both PBS and DMEM due to poor crosslinking. The swelling ratio first decreased along with increase of –CHO content, then increased. The swelling reached the minimum values for 3:1 hydrogel, revealing more crosslinking. In the case of PBS medium, the swelling value was 12.8 for 1:1 hydrogels, while it was 10.8 in DMEM. The relatively lower equilibrium swelling ratio in DMEM might be attributed to a great amount of amino acids, vitamins, glucose in the DMEM that form some hydrogen bonding and electrostatic attraction with glutamic acid repeating units in PLGA, thereby restricting the water uptake and swelling of the hydrogels.[48] Swelling ratio was also influenced by oxidation degree of PLGA-CHO, as displayed in Fig. 4c. It was greatly reduced with the increase of oxidation degree, which could be ascribed to the increasing amount of aldehyde groups and crosslinking density of the network. Low oxidation degree (≤10%) resulted in instability of the network and dissolution of the hydrogels after incubation in PBS solution. However, the hydrogels comprising same components were relatively stable in DMEM with a swelling ratio of 29.1, which was probably caused by the presence of various aforementioned chemicals, which might have hydrogen bonding and electrostatic attraction with polymer chains, prevent the water from contacting with polymer chain and decrease the breakage of network structure of the hydrogels.[48]

An appropriate degradation rate is necessary for injectable hydrogels in their application as cell delivery system in tissue engineering. Degradability of the hydrogels with different solid was investigated by examining the weight loss in PBS solution without and with papain (0.25mg/ml) addition, as shown in Fig. 4d1 and d2, respctively. In PBS solution without papain addition (Fig. 4d1), all of the hydrogels degraded relatively rapidly with a weight loss of 13~17 % within 3 days, presumably due to gel erosion and removal of the non-crosslinked macromolecular chains.[49] Then the degradation rate of PLGA hydrogel decreased gradually, which was caused by the breakage of the hydrazone bonds in between macromolecular chains. Within 7 weeks,

the hydrogels with the solid content of 3, 4, 5 and 6% showed the weight loss of 55, 44, 40 and 38%, respectively. Higher solid content contributed a higher resistance to biodegradability because of increased crosslinking density and compact network structure. As shown in Fig.4d2, with papain digestion, the weight loss for all of the hydrogels with different solid content occurred drastically within a short time (no more than 16h). An introduction of endopeptidase led to the rapid destruction of the network structure of the hydrogels and incision in chain segments to produce soluble fragments.[50]

3.4 Rheological properties of PLGA hydrogels

The rheological properties, which could give the information about the stability of three-dimensional crosslinked networks, were studied by oscillatory rheology. The frequency sweep measurements for the PLGA hydrogels after gelation were determined at 37 °C, and the results were expressed as storage modulus (G')/ loss modulus (G''), and $|\eta^*|$, as presented in Fig. 5.

For all the hydrogels, G'' was always lower than G', which was indicative of a stable crosslinked network. G' exhibited a plateau in the range 1–20 rad/s. The hydrogels with G' frequency independent feature also indicated an elastic behavior rather than fluid-like state. At higher frequencies, the macromolecular chain segments failed to rearrange themselves in the time scale of the imposed motion, and therefore stiffen up, which was characterized by an increase in G' and G''.[51-53]

G' increased rapidly with solid content and oxidation degree of PLGA-CHO, as shown in Fig. 5a and 5e. Hydrogels with a solid content of 6 wt % showed a 6~8 fold higher magnitude of G' compared to 3 wt % hydrogels. While G' increased 3~5 times when the oxidation degree of PLGA-CHO increased from 10 to 20%. The higher the solid content or the oxidation degree of PLGA-CHO, the higher the crosslinking degree, as the presence of a large number of reactive groups facilitated the gel formation and mechanical enhancement.[6] Also, $|\eta^*|$ increased rapidly with solid content (Fig. 5b) and oxidation degree of PLGA-CHO (Fig. 5f), which could be ascribed to the increase of crosslinking degree limited the relative movement between

macromolecular chains.

The G'/G'' of the hydrogels as a function of $–NH_2$ to –CHO molar ratio is displayed in Fig. 5c. The hydrogels exhibited higher value of G', when $-NH_2$ to -CHO molar ratio ranged from 1:1 to 3:1. It was reported that the gel rheological properties strongly depended on both the stoichiometric ratio and the molecular weight.[54] Higher crosslinking degree of PLGA hydrogels could be achieved at the condition of approximately equal number of $–NH_2$ and –CHO groups. Meanwhile, as the molecular weight of PLGA-ADH was significantly higher than that of PLGA-CHO, a certain degree of excess amount of PLGA-ADH was beneficial to improve the mechanical strength of PLGA hydrogels.

3.5 Micromorphology of PLGA hydrogels

Morphological characteristic of hydrogel is an important factor in terms of tissue engineering applications. The presence of porous structure is critical for tissue growth, cell adhesion and proliferation, as well as the diffusion of nutrients and oxygen.[55] As shown in Fig. 6, the inner pores of the hydrogels were irregular in shapes. The pore size of the hydrogel decreased rapidly from 25~160μm to 10~90μm, when the solid content increased from 3 to 6 wt % (Fig. 6a-e). Obviously, the micromorphology and pore size of PLGA hydrogels depended greatly on the solid content of the hydrogels, a higher solid content resulted in tighter network structure and the formation of smaller pore size in the hydrogels. Also, the internal morphology of the hydrogels was closely related to the molar ratio of $–NH_2$ to –CHO. The pore size first decreased, then increased with the increasing $–NH_2$/–CHO molar ratio (Fig. 6f-l). Additionally, some of the wall of the hydrogel with the $–NH_2$/–CHO molar ratio of 1:2 appeared to be torn during freeze-drying process, indicating an inadequate modulus to avoid the structural collapse during dehydration.

3.6 Distribution and ECM deposition of chondrocytes within PLGA hydrogels

Fluorescence microscopy and SEM observation were conducted to investigate whether the PLGA hydrogels could provide a suitable environment for harboring

chondrocytes.

As shown in Fig. 7a-d, fluorescent microscopy images of cells stained with the FDA/PI reagent illustrated that chondrocytes could tolerate 3D encapsulation and the injection of the PLGA hydrogels. Roundly shaped chondrocytes were uniformly distributed in the hydrogels. Majority of these cells were shown to survive after 3, 9, 14 and 21 days. Such a long survival period of 21d in the PLGA hydrogel is crucial for the injected cells to play their therapeutic role at the targeting position.[56]

The morphology of chondrocytes in the hydrogels was further observed by SEM equipped with a cold stage (temperature controlled sample holder, TCSH), which could expand sample flexibility and enable imaging of wet and beam-sensitive samples. After 1 d of culture, the chondrocytes with the size of 10−15 μm were uniformly distributed within the hydrogels (Fig. 7e and e′), and retained a nearly round shape, which was similar to that of native chondrocyte cells. After 3 and 5d of culture, the chondrocytes began to aggregate and deposit some extracellular matrix (ECM) (Fig. 7f, g and f′, g′). After 7 d, abundant ECM deposition was observed, covering the surface of cellular aggregates, as shown in Fig. 7h and h′. Our previous study also found the obvious deposition of ECM after 1 week seeding of adipose-derived stem cells onto the poly(L-glutamic acid)/chitosan scaffolds.[24]

3.7 Subcutaneously injection of PLGA hydrogels and ectopic cartilage formation

The hydrogels with chondrocytes encapsulated therein were transplanted into nude mice using double syringes, wherein one syringe was filled with PLGA-ADH solution containing the cell entity and the other with the PLGA-CHO solution. The mixing of the polymer solutions inside the hypodermic needle of the applicator led to gelation in a few seconds, allowing the placement of an insoluble hydrogel containing cell enitity inside the body. The hydrogel formed a bump at the implant site (Fig. 8a). For comparison, the suspensions of chondrocytes with same volume and cell density were also injected subcutaneously. The mice were cultured for 12 weeks (Fig. 8b) and then sacrificed. The newly generated cartilage-like tissues harvested from both the chondrocytes and chondrocytes/hydrogel groups exhibited a smooth surface,

semitransparent and white in color, as shown in Fig. 8c and d.

The average wet weight of the tissue generated from chondrocytes/hydrogel group was about 154mg, which was 73% higher than that for bare cells group (Fig. 8e). In histological evaluation, safranin-O (Fig. 8c1 and d1) and toluidine blue (Fig. 8c2 and d2) stain showed positive orange-red and blue staining respectively, denoting deposition of glycosaminoglycans (GAG) within the tissues-engineered cartilage. Immunohistochemical analysis (Fig. 8c3 and d3) with type II collagen antibody was strongly positive, demonstrating the cartilaginous tissue was rich in type II collagen.[57] The chondrocytes/hydrogel group exhibited more intense positive safranin-O and toluidine blue staining, indicating the neogenerated tissue was more mature with more deposition of typical ECM component, GAG and collagen II.[1]

4. Conclusions

Injectable poly(L-glutamic acid) (PLGA) hydrogels were designed for cartilage tissue engineering. The hydrazide-modified poly(L-glutamic acid) (PLGA-ADH) and aldehyde-modified poly(L-glutamic acid) (PLGA-CHO) were prepared by using EDC activation and $NaIO_4$ oxidation. The mixing of solutions of PLGA-ADH and PLGA-CHO resulted in intermacromolecular Schiff base crosslinking reaction and rapid formation of hydrogels at physiological condition. The gelation time, equilibrium swelling, degradation rate, microscopic morphology, and rheological properties could be easily controlled by the solid content of the hydrogels, $–NH_2$/–CHO molar ratio and oxidation degree of PLGA-CHO. Encapsulation of chondrocytes in the PLGA hydrogels demonstrated that the majority of cells were viable and deposited abundant ECM. A preliminary study exhibited injectability and rapid in vivo gel formation, as well as cell ingrowth and ectopic chondrogenesis. Taken together, these results have indicated that PLGA injectable hydrogel is a prospective candidate as an injectable cell carrier and may have potential uses in cartilage regeneration using minimally invasive techniques.

Acknowledgments

The work was supported by the National Natural Science Foundation of China (Nos. 51473090 and 51373094), the Natural Science Foundation of Shanghai City (No. 14ZR1414600), and the Science and Technology Commission of Shanghai Municipality (No. 15JC1490400). Mr. Yuliang Chu from Instrumental Analysis Research Centre (Shanghai University) is acknowledged for their help in SEM measurement.

References

1 H. Park, B. Choi, J. Hua and M. Lee, *Acta Biomater*., 2013, **9**, 4779–4786.

2 T. D. Sargeant, A. P. Desai, S. Banerjee, A. Agawu and J. B. Stopek, *Acta Biomater*., 2012, **8**, 124–132.

3 R. Jin, L. S. Moreira Teixeira, P. J. Dijkstra, C. A. van Blitterswijk, M. Karperien and J. Feijen, *Biomaterials*, 2010, **31**, 3103–3113.

4 D. Mortisen, M. Peroglio, M. Alini and D. Eglin, *Biomacromolecules*, 2010, **11**, 1261−1272.

5 J. J. Guan, Y. Hong, Z. W. Ma and W. R. Wagner, *Biomacromolecule*, 2008, **9**, 1283−1292.

6 B. Balakrishnan and A. Jayakrishnan, *Biomaterials*, 2005, **26**, 3941−3951.

7 C. K. Kuo and P. X. Ma, *Biomaterials*, 2001, **22**, 511−521.

8 S. J. de Jong, S. C. De Smedt, J. Demeester, C. F. van Nostrum, J. J. Kettenes-van den Bosch and W. E. Hennink, *J. Controlled Release*, 2001, **72**, 47−56.

9 G. W. Bos, W. E. Hennink, L. A. Brouwer, W. den Otter, T. F. J. Veldhuis, C. F. van Nostrum and M. J. A. van Luyn, *Biomaterials,* 2005, **26**, 3901−3909.

10 S. A. Robb, B. H. Lee, R. McLemore and B. L. Vernon, *Biomacromolecules*, 2007, **8**, 2294−2300.

11 P. Y. W. Dankers, M. C. Harmsen, L. A. Brouwer, M. J. A. van Luyn and E. W. Meijer, *Nat. Mater*., 2005, **4**, 568−574.

12 M. Kurisawa, F. Lee, L. S. Wang and J. E. Chung, *J. Mater. Chem*., 2010, **20**, 5371−5375.

13 S. Y. Lee and G. Tae, *J. Controlled Release*, 2007, **119**, 313−319.

14 H. P. Tan, C. R. Chu, K. A. Payne and K. G. Marra, *Biomaterials*, 2009, **30**, 2499−2506.

15 N. E. Fedorovich, M. H. Oudshoorn, D. van Geemen, W. E. Hennink, J. Alblas and W. J. A. Dhert, *Biomaterials*, 2009, **30**, 344–353.

16 K. Matsumura, N. Nakajima, H. Sugai and S. H. Hyon, *Carbohydr. Polym.*, 2014,

113, 32−38.

17 D. A. Wang, S. Varghese, B. Sharma, I. Strehin, S. Fermanian, J. Gorham, H. D. Fairbrother, B. Cascio, J. H. Elisseeff, *Nat. Mater*. 2007, **6**, 385−392.

18 M. K. Nguyen and E. Alsberg, *Prog. Polym. Sci.*, 2014, **39**, 1235–1265.

19 B. Balakrishnan and A. Jayakrishnan, *Biomaterials*, 2005, **26**, 3941–3951.

20 D. A. Ossipov, K. Brannvall, K. Forsberg-Nilsson and J. Hilborn, *J. Appl. Polym. Sci*., 2007, **106**, 60−70.

21 E. B. Hunziker, *Osteoarthritis Cartilage*, 2002,**10**, 432–463.

22 C. Li, *Adv. Drug Delivery Rev*., 2002, **54**, 695−713.

23 S. F. Yan, K. X. Zhang, Z. W. Liu, X. Zhang, L. Gan, B. Cao, X. S. Chen and J. B. Yin, *J. Mater. Chem. B*, 2013, **1**, 1541−1551.

24 K. X. Zhang, Y. Zhang, S. F. Yan, L. L. Gong, J. Wang, X. S. Chen, L. Cui and J. B. Yin, *Acta Biomater*., 2013, **9**, 7276−7288.

25 J. Maia, L. Ferreira, R. Carvalho, M. A. Ramos and M. H. Gil, *Polymer*, 2005, **46**, 9604−9614.

26 T. Ito, Y. Yeo, C. B. Highley, E. Bellas and D. S. Kohane, *Biomaterials*, 2007, **28**, 975−983.

27 C. Gentilini, Y. Dong, J. R. May, S. Goldoni, D. E. Clarke, B. H. Lee, E. T. Pashuck and M. M. Stevens. *Adv. Healthcare Mater*. 2012, **1**, 308−315.

28 X. He and E. Jabbari. *Biomacromolecules,* 2007, **8**, 780−792.

29 P. Y. Ni, Q. X. Ding, M. Fan, J. F. Liao, Z. Y. Qian, J. C. Luo, X. Q. Li, F. Luo, Z. M. Yang and Y. Q. Wei. *Biomaterials*, 2014, **35**, 236−248.

30 S. J. Buwalda, L. Calucci, C. Forte, P. J. Dijkstra and J. Feijen. *Polymer,* 2012, **53**, 2809–2817.

31 A. Alexander, Ajazuddin, J. Khan, S. Saraf and S. Saraf. *J. Controlled Release*, 2013, **172**, 715–729.

32 A. Abarrategi, Y. Lópiz-Morales,, V. Ramos, A. Civantos, L. López-Durán, F. Marco and J. L. López-Lacomba. *J. Biomed. Mater. Res.*, 2010, **95**, 1132–1141.

33 P. Markland, G. L. Amidon and V. C. Yang, *Int. J. Pharm.*, 1999, **178**, 183–192.

34 Z. J. Song, J. B. Yin, K. Luo, Y. Z. Zheng, Y. Yang, Q. Li, Y. Yang, S. F. Yan and

X. S. Chen. *Macromol. Biosci.*, 2009, **9**, 268−78.

35 B. Cao, S. F. Yan, L. Cui, X. S. Chen and Y. T. Xie, *Macromol. Biosci*., 2011,**11**, 427−34.

36 W. Y. Su, Y. C. Chen and F. H. Lin, *Acta Biomater*., 2010, **6**, 3044−3055.

37 X. Jia, G. Colombo, R. Padera, R. Langer and D. S. Kohanee, *Biomaterials*, 2004, **25**, 4797−4804.

38 E. F. Vieira, A. R. Cestari, C. Airoldi and W. Loh, *Biomacromolecules*, 2008, **9**, 1195−1199.

39 C. Hiemstra, L. J. van der Aa, Z. Zhong, P. J. Dijkstra and J. Feijen. *Biomacromolecules*, 2007, **8**, 1548–1556.

40 L. S. M. Teixeira, S. Bijl, V. V. Pully, C. Otto, R. Jin, J. Feijen, C. A. van Blitterswijk and P. J. Dijkstra, *Biomaterials*, 2012, **33**, 3164–3174.

41 X. Jia, Y. Yeo, R. J. Clifton, T. Jiao, D. S. Kohane, J. B. Kobler, S. M. Zeitels and R Langer, *Biomacromolecules*, 2006, **7**, 3336–3344.

42 Y. Jiao, D. Gyawali, J. M. Stark, P. Akcora, P. Nair, R. T. Tran and J. Yang, *Soft Matter*, 2012, **8**, 1499−1507.

43 A. Fathi, S. M. Mithieux, H. Wei, W. Chrzanowski, P. Valtchev, A. S. Weiss and F. Dehghani, *Biomaterials*, 2014, **35**, 5425−5435.

44 N. Annabi, A. Fathi, S. M. Mithieux, P. Martens, A. S. Weiss and F. Dehghani, *Biomaterials*, 2011, **32**, 1517−1525.

45 Y. Zhang, C. Y. Won and C. C. Chu, *J. Polym. Sci. Pol. Chem.*, 1999, **37**, 4554–4569.

46 H. Park, X. Guo, J. S. Temenoff, Y. Tabata, A. I. Caplan, F. K. Kasper and A. G. Mikos, *Biomacromolecules*, 2009, **10**, 541–546.

47 Z. E. Meybodi, M. Imani and M. Atai, *Carbohyd. Polym*. 2013, **92**, 1792–1798.

48 F. Xiao, L. Chen, R. F. Xing, Y. P. Zhao, J. Dong, G. Guo and R. Zhang, *Colloid. Surfaces B.*, 2009, **71**, 13−18.

49 M. C. Tate, D. A. Shear, S. W. Hoffman, D. G. Stein and M. C. LaPlaca, *Biomaterials*, 2001, **22**, 1113–1123.

50 Y. Yoshida, K. Makino, T. Ito, Y. Yamakawa and T. Hayashi. *Eur. Polym. J.*, 1996,

32, 877−881.

51 M. J. Moura, M. M. Figueiredo, M. H. Gil, *Biomacromolecules*, 2007, **8**, 3823–3829.

52 D. Teng, Z. Wu, X. Zhang, S. Zhang, C. Zheng and Z. Wang, C. Li, *Polymer*, 2010, **51**, 639–646.

53 M. A. Abed and H. B. Bohidar, *Eur. Polym. J.*, 2005, **41**, 2395–2405.

54 A. Izuka, H. H. Winter and T. Hashimoto, *Macromolecules*, 1992, **25**, 2422–2428.

55 Y. X. Dong, A. O. Saeed, W. Hassan, C. Keigher, Y. Zheng, H. Y. Tai, A. Pandit and W. X. Wang, *Macromol. Rapid Commun*. 2012, **33**, 120−126.

56 B. Yang, Y. L. Zhang, X. Y. Zhang, L. Tao, S. X. Lia and Y. Wei, *Polym. Chem.*, 2012, **3**, 3235–3238.

57 B. H. I. Ruszymah, B. S. Lokman, A. Asma, S. Munirah, K. Chua, A. L. Mazlyzam and M. R. Isa, N. H. Fuzina, B. S. Aminuddin, *Int. J. Pediatr. Otorhi.* 2007, **71**, 1225–1234.

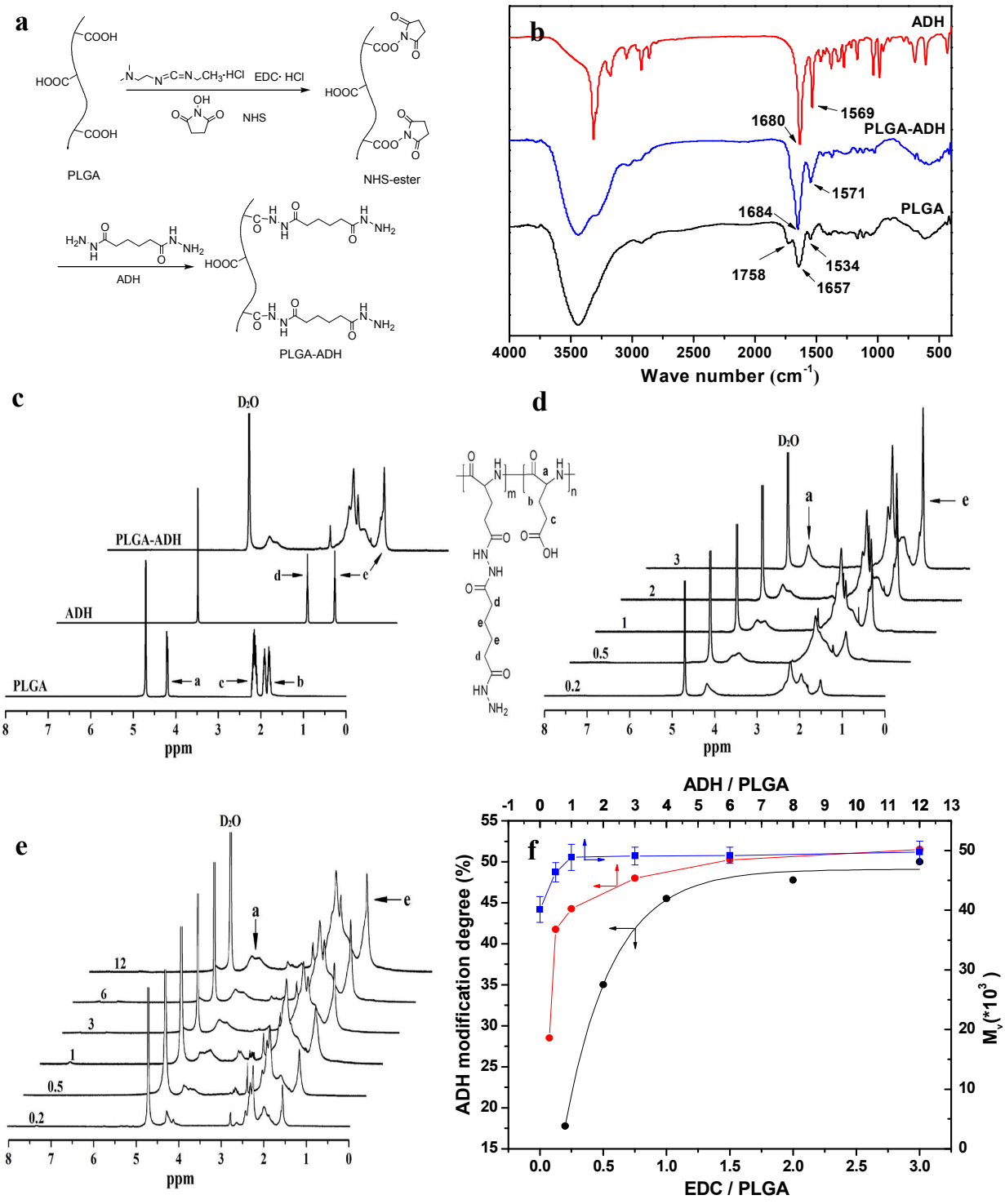

Fig. 1 Synthesis and characterization of PLGA-ADH. (a) Schematic representation of ADH modification. (b) FTIR spectra, (c) ^{1}H NMR spectra of ADH, PLGA and PLGA-ADH. ^{1}H NMR spectra of PLGA-ADH obtained by using different amount of (d) EDC and (e) ADH. The numbers indicate different (d) EDC/PLGA and (e) $–NH_2$/–CHO molar ratios. (f) ADH modification degree and molecular weight of PLGA-ADH as a function of EDC and ADH amount.

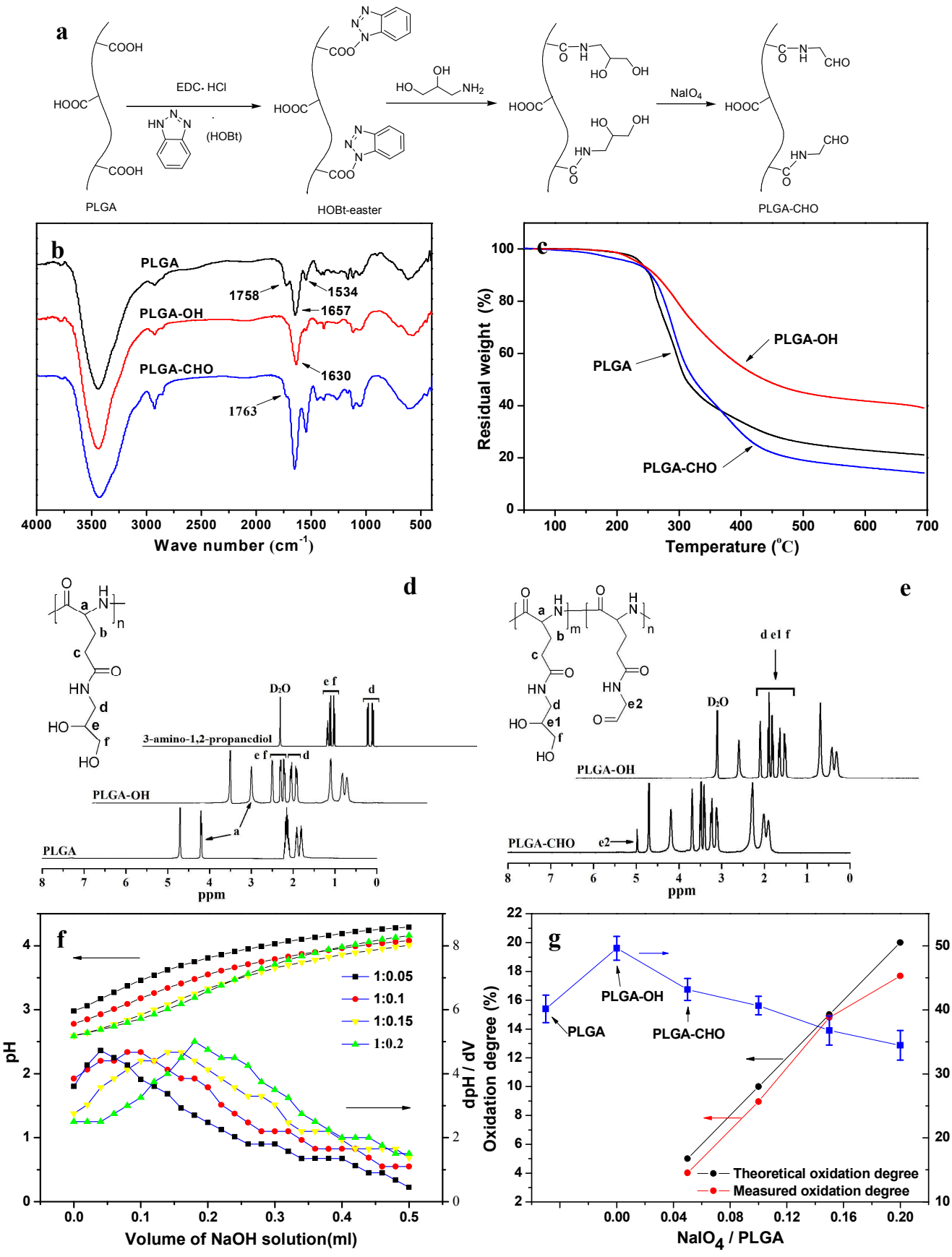

Fig. 2 Synthesis and characterization of PLGA-CHO. (a) Schematic representation of modification with 3-amino-1,2-propanediol and oxidation reaction. (b) FTIR spectra and (c) TGA curves of PLGA, PLGA-OH and PLGA-CHO. (d-e) ^{1}H NMR spectra of 3-amino-1,2-propanediol, PLGA, PLGA-OH and PLGA-CHO. (f) Hydroxylamine hydrochloride potentiometric titration of various PLGA-CHO samples. (g) The molecular weight, theoretical and measured oxidation degree of PLGA-CHO as a function of $NaIO_4$ amount.

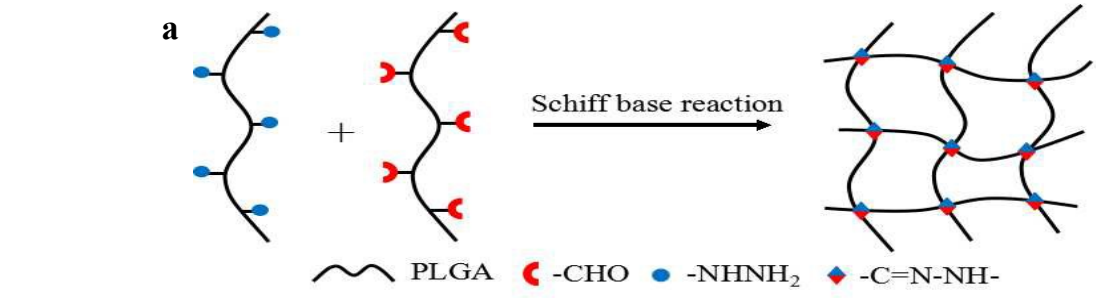

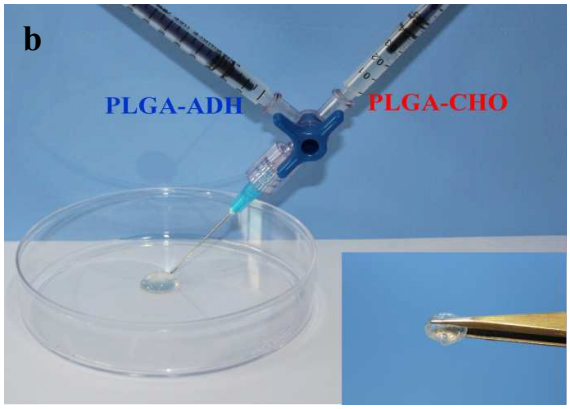

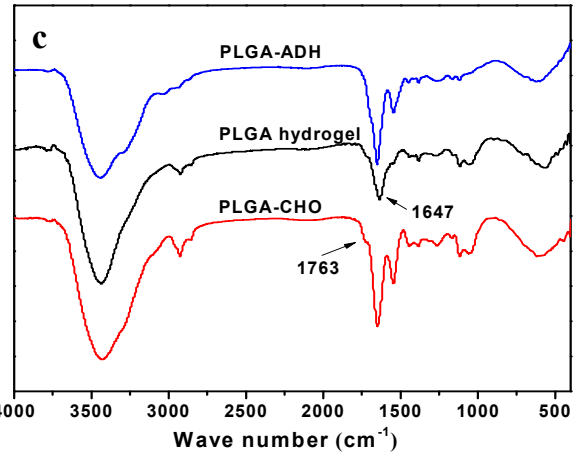

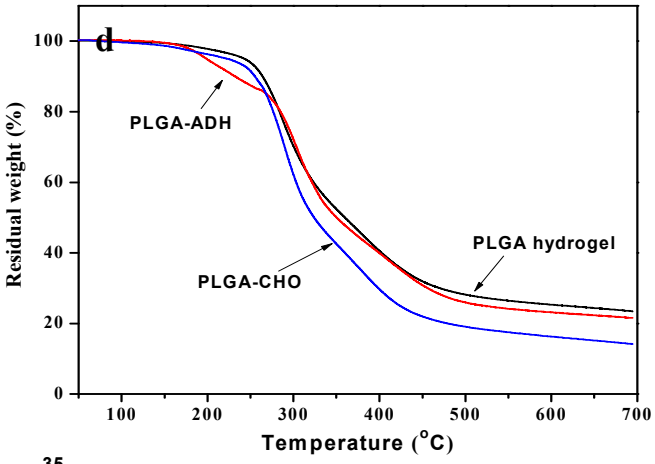

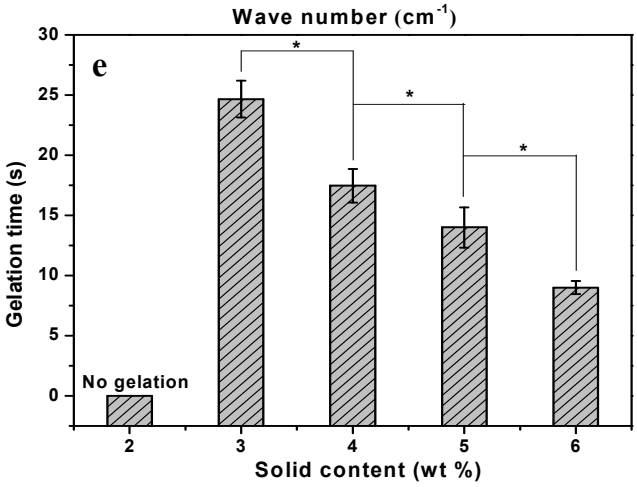

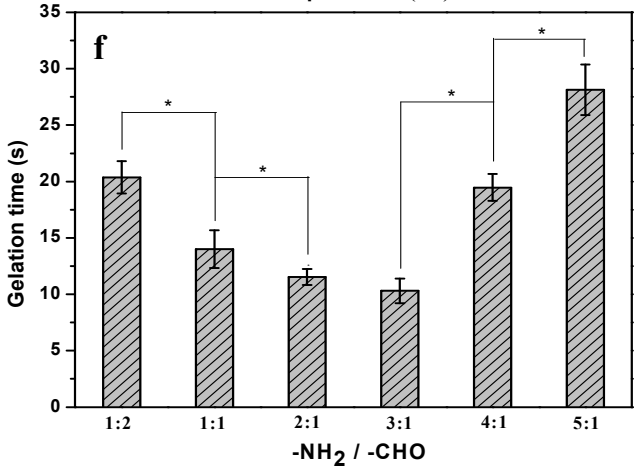

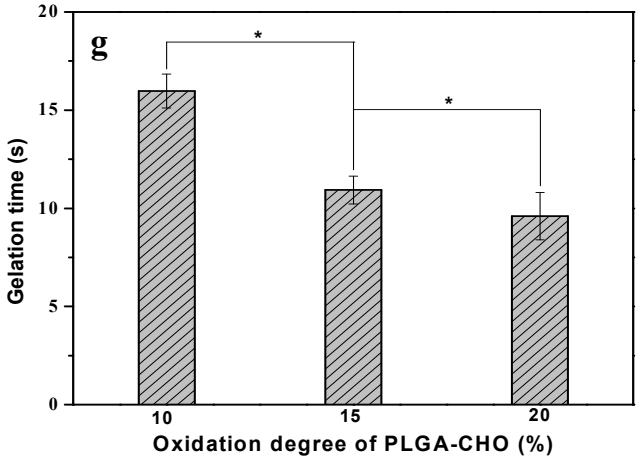

Fig. 3 Hydrogel formation and gelation time. (a) Schematic illustration of in situ hydrogel crosslinking by Schiff base reaction. (b) Images of the in situ formation of PLGA hydrogel using dual syringes. (c) FTIR spectra and (d) TGA curves of PLGA-ADH, PLGA-CHO, and PLGA hydrogel. (e) Gelation time of PLGA hydrogels with different solid contents (n = 3, $*p < 0.05$). $–NH_2$/–CHO molar ratio was set at 1:1. (f) Gelation time of PLGA hydrogels as a function of $–NH_2$/–CHO molar ratios (n = 3, $*p < 0.05$). The solid content of PLGA hydrogels was fixed at 5 wt%. (g) Gelation time of PLGA hydrogels using PLGA-CHO with different oxidation degrees ($–NH_2$/–CHO molar ratio =1:1, solid content of PLGA hydrogels = 5 wt%, n = 3, $*p < 0.05$).

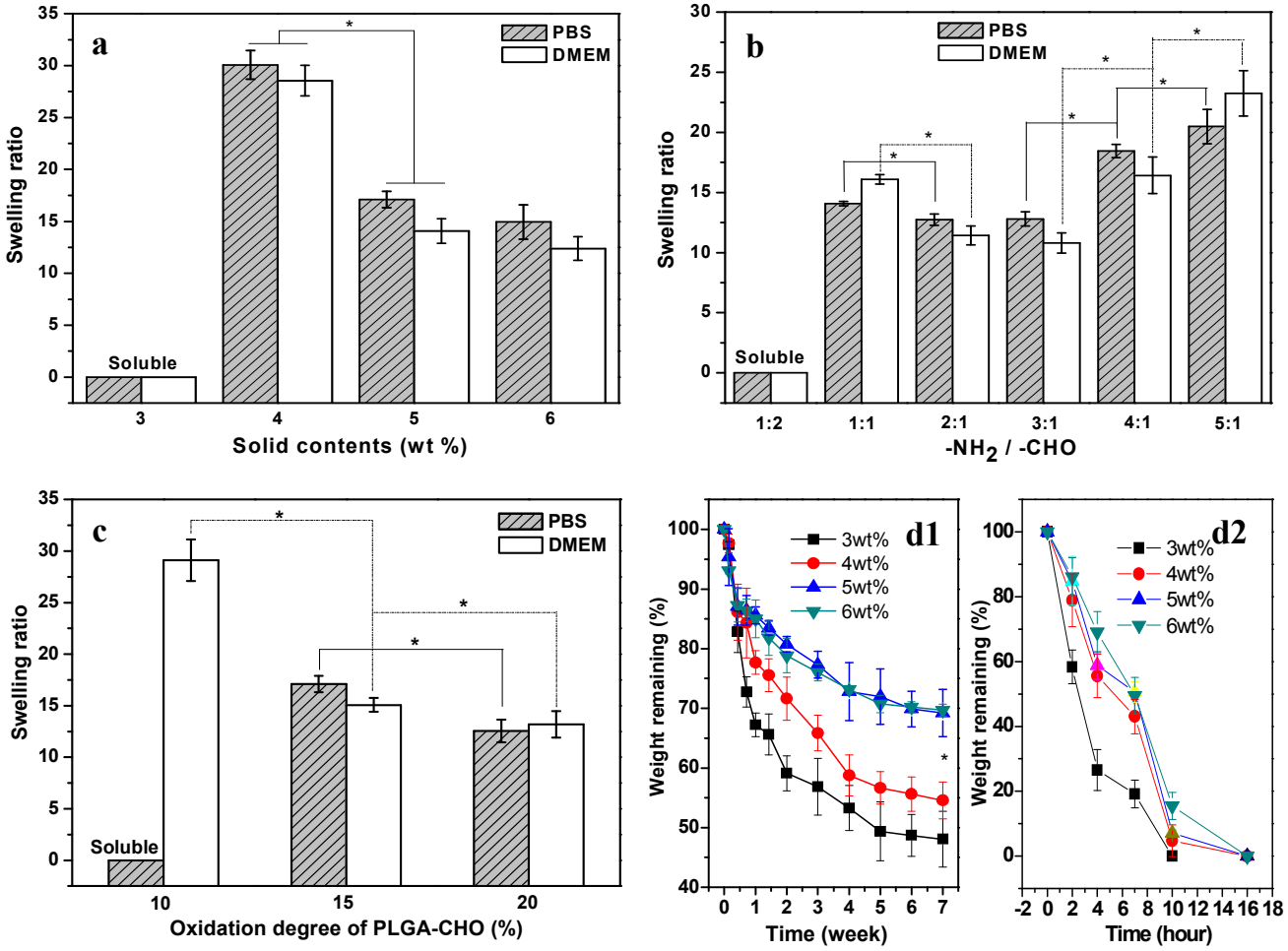

Fig. 4 Equilibrium swelling and degradation behavior of the hydrogels. Equilibrium swelling of the hydrogels as a function of (a) solid content, (b) $–NH_2$/–CHO molar ratio, and (c) oxidation degree of PLGA-CHO (n = 3, $*p < 0.05$). As indicated in the figures, some of hydrogels were soluble during the incubation period. (d) In vitro degradation of the hydrogels with different solid contents in PBS solution (d1) and PBS containing 0.25mg/ml papain (d2) (n = 3, $*p < 0.05$).

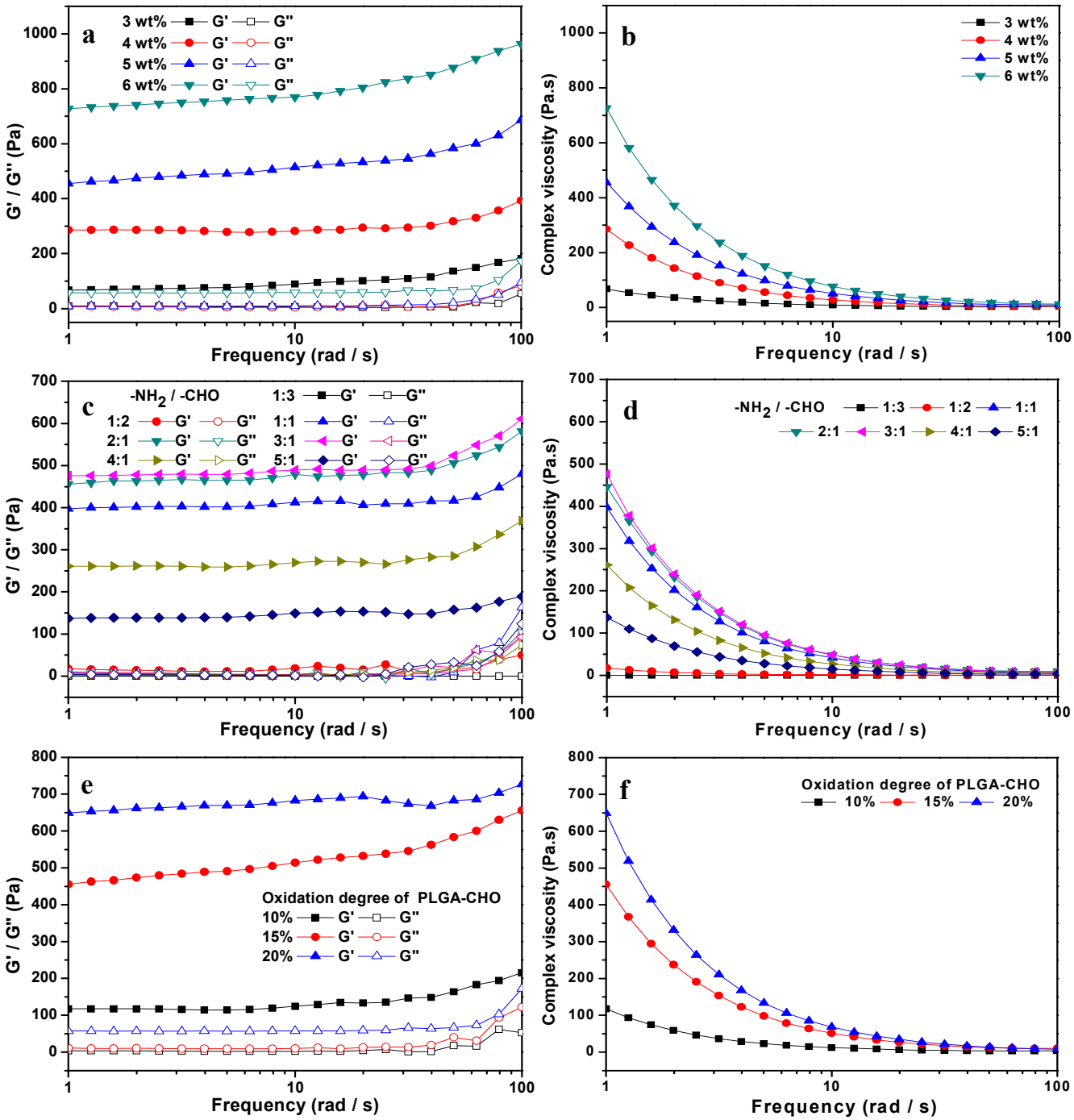

Fig. 5 Rheological properties of PLGA hydrogels. Frequency dependence of storage modulus/loss modulus (G'/G'') and complex viscosity $|\eta^*|$ for PLGA hydrogels with different (a-b) solid contents, (c-d) $–NH_2/–CHO$ molar ratios, and (e-f) oxidation degrees of PLGA-CHO.

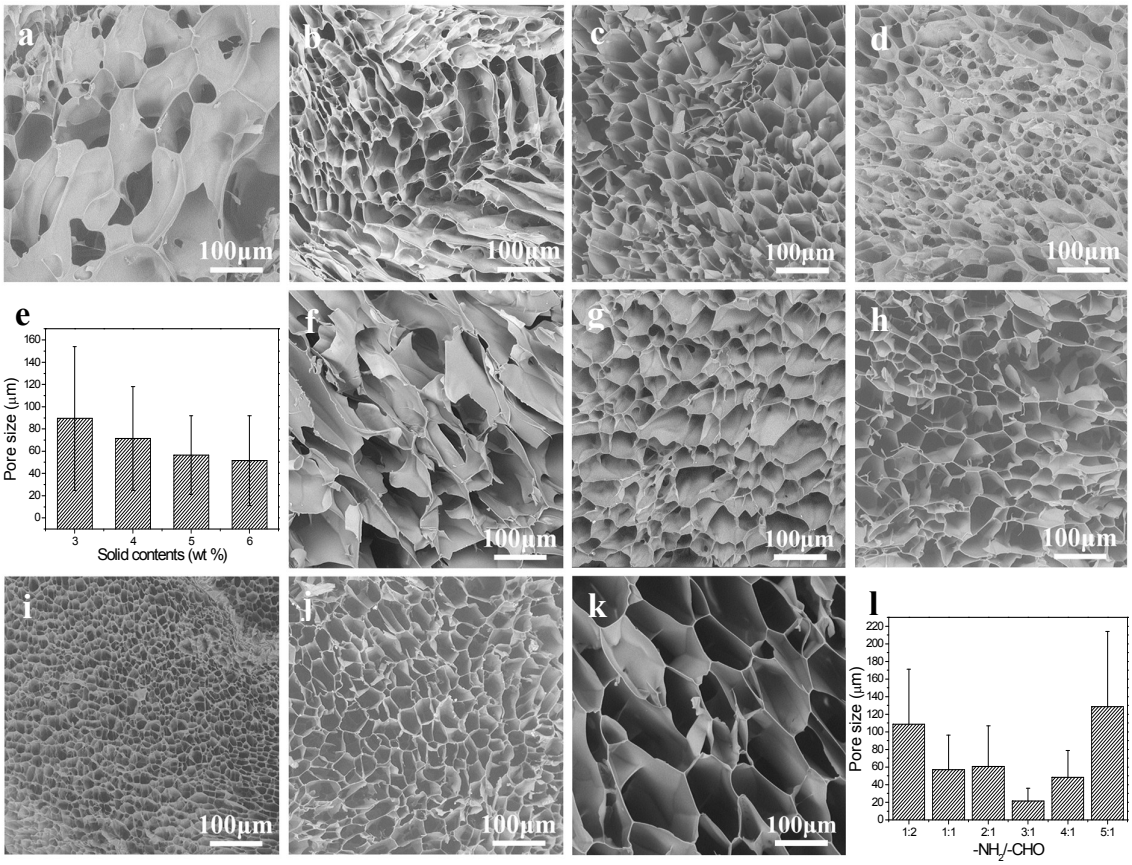

Fig. 6 SEM images of the hydrogels with different solid contents: (a) 3, (b) 4, (c) 5, and (d) 6 wt %. (e) Effect of solid content on the pore size of the PLGA hydrogels. SEM images of PLGA hydrogels with different $–NH_2$/–CHO molar ratios: (f) 1:2, (g) 1:1, (h) 2:1, (i) 3:1, (j) 4:1 and (k) 5:1. (l) Effect of $–NH_2$/–CHO molar ratios on the pore size of the PLGA hydrogels.

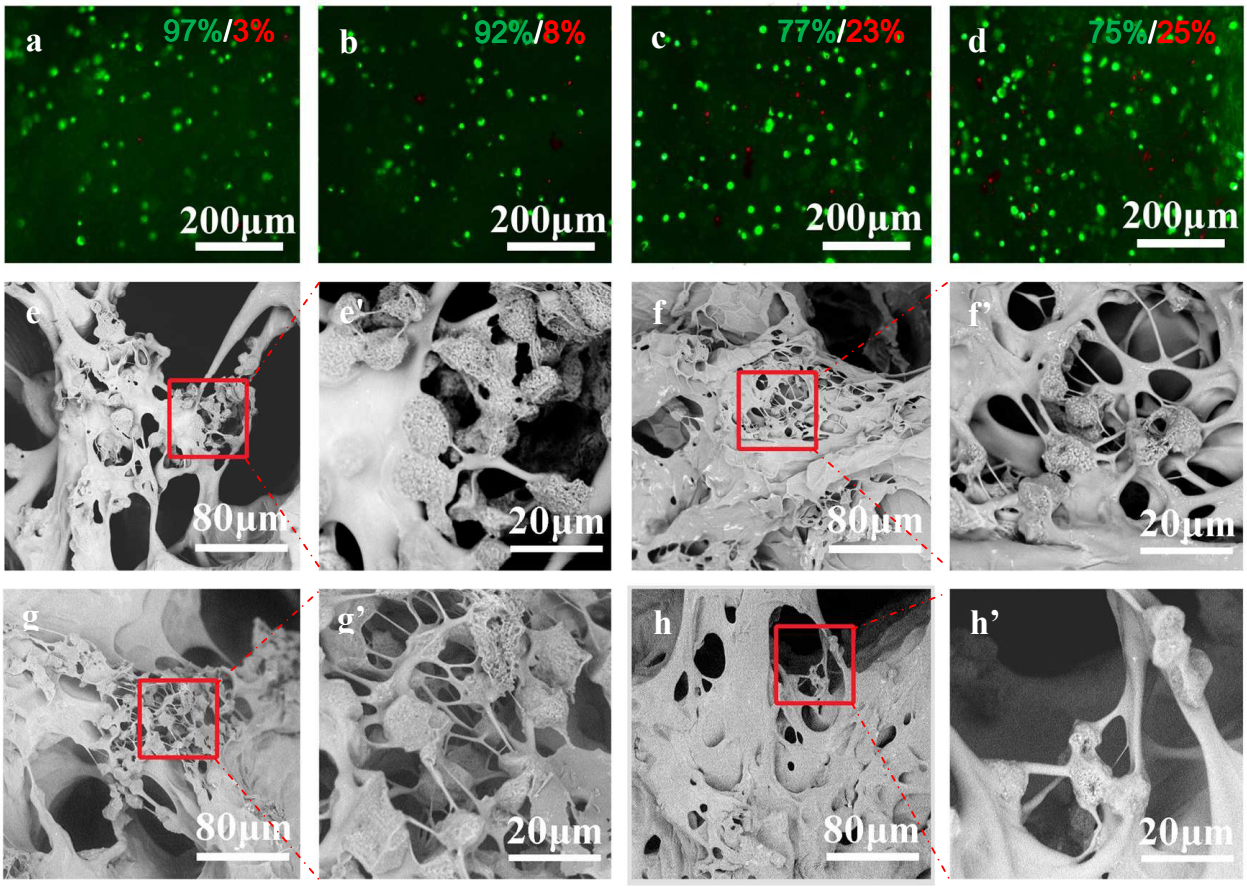

Fig. 7 Cytoviability assay. Fluorescence micrographs of the chondrocytes encapsulated in PLGA hydrogels at different times of culture: (a) 3, (b) 9, (c) 14, and (d) 21d. The living cells were stained with FDA (green) and the dead cell nuclei were stained with PI (red), and living/dead cell percentages are labeled on the top right corner of the each figure. SEM images of the chondrocytes encapsulated in PLGA hydrogels at different times of culture: (e) 1, (f) 3, (g) 5, and (h) 7d. High magnification SEM images of the boxed regions of (e−h) are shown in (e′−h′), respectively.

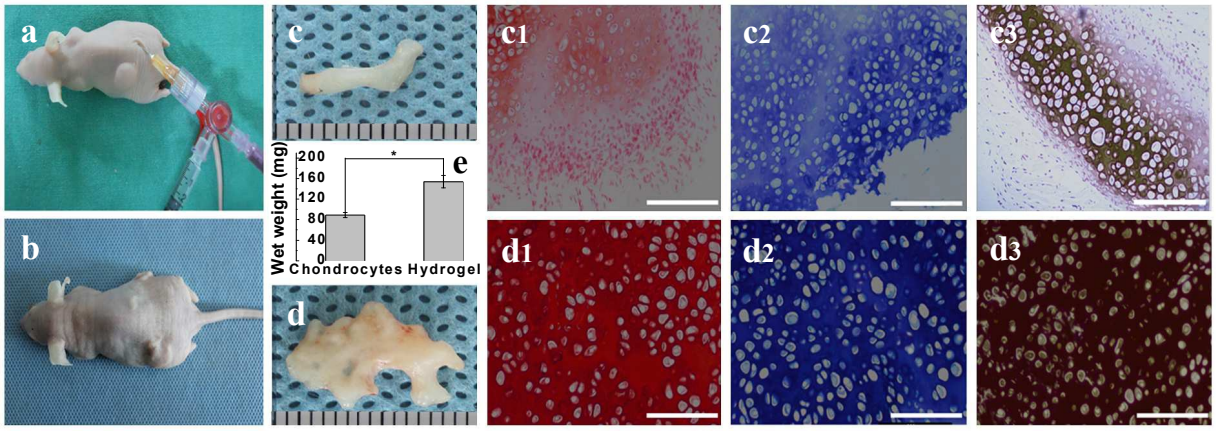

Fig. 8 Comparison of PLGA hydrogel as cell carriers and bare cell suspension for cartilage regeneration in vivo. Subcutaneous injection of 5 wt% hydrogels into athymic nude mice: (a) during injection, (b) after 12 weeks. Newly generated cartilageous tissues harvested after 12 weeks subcutaneous injection and corresponding tissue mass and biochemical compositions: (c, c1, c2, c3) bare cells, (d, d1, d2, d3) chondrocytes encapsulated in PLGA hydrogels. (c, d) Newly generated cartilageous tissues, (e) tissue mass ($n = 3$, $^*p < 0.05$), (c1,d1) safranin-O staining, (c2, d2) toluidine blue staining, and (c3, d3) immunohistochemical staining, respectively (bar scales: 200 μm).